Controlling Substitution Chemistry in Ruthenium(II) Systems. Synthesis of Heteroleptic Complexes Incorporating the $[Ru([9]aneS_3)]^{2+}$ Metal Center

Sue Roche, Harry Adams, Sharon E. Spey, and James A. Thomas*

Department of Chemistry, University of Sheffield, Sheffield S3 7HF, U.K.

Received November 17, 1999

The complex $[Ru(py)_3([9]aneS_3)][PF_6]_2$, **1** (py = pyridine), has proved to be a suitable starting material for the synthesis of heteroleptic Ru(II) complexes. By exploiting unfavorable steric interactions between 2-H and 6-H hydrogens of coordinated pyridyl ligands, we have synthesized half-sandwich complexes incorporating the thiocrown $[9]aneS_3$ and a variety of facially coordinated N-donor ligands. Such complexes are easily prepared: Stirring **1** at room temperature in the presence of a suitable nitrile ligand leads to the exclusive substitution of one py ligand to produce complexes such as $[([9]aneS_3)Ru(py)_2(NCMe)][PF_6]_2$, **2**. However, if the same reaction is carried out at higher temperatures, two py ligands are substituted, leading to complexes such as $[([9]aneS_3)Ru(py)(NCMe)_2][PF_6]_2$, **3**. An alternative approach to such heteroleptic species has also been developed which exploits the restricted ability of thioethers to neutralize positive charges through σ-donation. This phenomenon allows the synthesis of heteroleptic complexes in a two-step procedure via monocationic species. By variation of the donor/acceptor properties of ligands incorporated into the $[Ru([9]aneS_3)]^{2+}$ metal center, it is possible to tune the Ru(III)/Ru(II) redox couple over a range of >700 mV. The solid-state structures of **1**−**3** were confirmed by X-ray crystallography studies. Crystal data: $C_{22}H_{30}F_{12}N_4O_2P_2RuS_3$ (**1**·CH_3NO_2), monoclinic, *Cc*, $a = 23.267(5)$ Å, $b = 11.5457(18)$ Å, $c = 26.192(5)$ Å, $\alpha = 90°$, $\beta = 114.836(10)°$, $\gamma = 90°$, $Z = 8$; $C_{18}H_{25}F_{12}N_3P_2RuS_3$ (**2**), triclinic, $P\bar{1}$, $a = 11.3958(19)$ Å, $b = 11.4280(19)$ Å, $c = 11.930(2)$ Å, $\alpha = 100.518(3)°$, $\beta = 100.542(3)°$, $\gamma = 112{,}493(3)°$, $Z = 2$; $C_{15}H_{23}F_{12}N_3P_2RuS_3$ (**3**), orthorhombic, $Pna2_1$), $a = 14.748(5)$ Å, $b = 18.037(18)$ Å, $c = 10.341(5)$ Å, $\alpha = 90°$, $\beta = 90°$, $\gamma = 90°$, $Z = 4$.

Introduction

Over the past 30 years, there has been continuous research into ruthenium(II) complexes based on $[Ru(bpy)_3]^{2+}$ and $[Ru(NH_4)_n]^{2+}$.[1−3] Such systems have played an important part in the development of devices for molecular electronics,[4] forming the basic components of molecular wires and molecular switches.[5,6] Changing the ligands on the metal center can have a significant effect on the electrochemical and/or electron-transfer properties of a metal complex.[7,8] Hence, the synthesis of truly functional molecular assemblies often requires precise control over the substitution chemistry around such Ru(II) metal centers.[9]

Previous research has involved using nitrogen-based ligands, such as NH_3 and 2,2′-bipyridine (bpy), coordinated to the metal ion. Our attempt has been to broaden the experimental basis of such work by introducing new metal complexes incorporating sulfur-donor ligands. The first steps in such work has focused on the readily available thiamacrocycle $[9]aneS_3$. Previously, the fragment $[Ru([9]aneS_3)]^{2+}$ was used to construct electron-transfer systems[10] and supramolecular architectures.[11] As part of a long-term aim to create molecular devices with targeted coordination geometries, the substitution chemistry of the above fragment is being further investigated.

Previous synthetic strategies for the synthesis of heteroleptic ruthenium(II) complexes have involved using bidentate[12,13] and tridentate[14] ligands. Using the previously reported $[Ru(DMSO)Cl_2([9]aneS_3)]$,[15] we have developed a methodology to control the substitution chemistry of facially coordinated N-donor ligands around the $[Ru([9]aneS_3)]^{2+}$ metal center. Here, we report the synthesis of the piano stool complex $[Ru(py)_3([9]aneS_3)]^{2+}$, (py = pyridine), which has proved to be a favorable intermediate in the preparation of heteroleptic ruthenium(II) complexes incorporating monodentate N-donor ligands. We have also synthesized heteroleptic compounds from $[Ru(DMSO)Cl_2([9]aneS_3)]$ in a two-step process via the bis-(pyridyl) intermediate $[Ru(py)_2Cl([9]aneS_3)]^+$.

* Corresponding author. E-mail: james.thomas@sheffield.ac.uk.

(1) Juris, A.; Balzani, V. *Coord. Chem. Rev.* **1998**, *84*, 85.
(2) Balzani, V.; Juris, A.; Venturi, M.; Campagna, S.; Serroni, S. *Chem. Rev.* **1996**, *96*, 759.
(3) Collin, J.-P.; Gavina, G.; Heltz V.; Sauvage, J.-P. *Eur. J. Inorg. Chem.* **1998**, 1.
(4) Meria, E.; Amouyal, E. *Inorg. Chem.* **1996**, *35*, 2212.
(5) Balzani, V.; Scandola, F. *Supramolecular Photochemistry*; Ellis Horwood: Chichester, England, 1991.
(6) Sauvage, J.-P.; Collin, J.-P.; Chambron, J.-C.; Guillerez, S.; Coudret, C. *Chem. Rev.* **1994**, *94*, 993.
(7) Crutchley, R. J. *Adv. Inorg. Chem.* **1994**, *41*, 273.
(8) Amouyal, E. *Sol. Energy Mater. Sol. Cells* **1995**, *38*, 249.
(9) Sullivan, B. P.; Calvert, J. M.; Meyer, T. J. *Inorg. Chem.* **1980**, *19*, 1404.
(10) Roche, S.; Yellowlees, L. J.; Thomas, J. A. *J. Chem. Soc., Chem. Commun.* **1998**, 1429.
(11) Roche, S.; Haslam, C.; Adams, H.; Heath, S. L.; Thomas, J. A. *J. Chem. Soc., Chem. Commun.* **1998**, 1681.
(12) Amouyal, E.; Penaud-Berruyer, F.; Azhari, D.; Ait-Haddou, H.; Fontanas, C.; Bejan, E.; Daran, J.-C.; Balavoine, G. G. A. *New J. Chem.* **1998**, 373.
(13) (a) Strouse, G. F.; Anderson, P. A.; Schoonover, J. R.; Meyer, T. J.; Keene, F. R. *Inorg. Chem.* **1992**, *31*, 3004. (b) Anderson, P. A.; Deacon, G. B.; Haarmann, K. H.; Keene, F. R.; Meyer, T. J.; Reitsma, D. A.; Skelton, B. W.; Strouse, G. F.; Thomas, N. C.; Treadway, J. A.; White, A. H. *Inorg. Chem.* **1995**, *34*, 6145.
(14) Fallahpour, R. A. *Eur. J. Inorg. Chem.* **1998**, 1205.
(15) Landrafe, C.; Sheldrick, W. S. *J. Chem. Soc., Dalton Trans.* **1994**, 1885.

10.1021/ic991336g CCC: $19.00
Published on Web 05/12/2000

By variation of the ligand substitution pattern around the $[Ru([9]aneS_3)]^{2+}$ metal center, it is possible to tune the physical properties of this metal center. For example, by adjustment of the donor/acceptor properties of coordinated ligands incorporated in such complexes, the Ru(III)/Ru(II) electrochemical couple can be shifted over a range of >700 mV.

Experimental Section

Materials and Procedures. The complex $[Ru(DMSO)Cl_2([9]aneS_3)]$ was prepared according to a previously published procedure.[15] All other reagents were obtained commercially and used as supplied. All reactions were conducted under an atmosphere of nitrogen. Products were dried at room temperature in a vacuum desiccator for ca. 10 h prior to characterization.

Physical Measurements. ^{1}H NMR spectra were recorded on a Bruker AM250 spectrometer operating in the Fourier transform mode and were acquired in a range of 1−12 ppm with 32K data points. UV/vis spectra were recorded on a Unicam UV2 UV/vis spectrometer. Elemental analyses were obtained on a Perkin-Elmer 2400 analyzer operating at 975 °C. Cyclic voltammetric measurements were carried out using an EG&G 253 potentiostat controlled by 270 Electrochemical Research Software. A three-electrode cell was used with an Ag^+/AgCl reference electrode separated from a Pt disk working electrode and Pt wire auxiliary electrode. Tetra-*n*-butylammonium hexafluorophosphate, 0.1 M in acetonitrile, doubly recrystallized from ethyl acetate/diethyl ether, was used as the supporting electrolyte. A scan rate of 200 mV s^{-1} was employed.

Syntheses. $[([9]aneS_3)Ru(py)_3][PF_6]_2$, 1. To a solution of 0.215 g (0.5 mmol) of $[Ru(DMSO)Cl_2([9]aneS_3)]$ in 20 mL of 1:1 ethanol/water was added $AgNO_3$ (0.170 g, 2 equiv), and the reaction mixture was refluxed for 3 h. After removal of AgCl by filtration, excess pyridine (1 mL) was added and the mixture was refluxed for 3 h. On cooling, NH_4PF_6 (0.245 g, 3 equiv) was added and the resulting mixture was allowed to stand overnight. The resultant precipitate was washed sequentially with water and ethanol and then dried in vacuo, yielding 0.33 g (82%) of **1** as a green powder. ^{1}H NMR ($(CD_3)_2CO$): δ 2.92−3.16 (m, 12H), 7.57−7.64 (m, 6H), 8.12 (tt, J = 7.63 and 1.53, 3H), 8.64 (dd, J = 6.40 and 1.53, 6H). (All J values are given in hertz, here and elsewhere.) FAB MS, *m*/*z* (%): 664 (15) [$M^+ - PF_6$], 518 (5) [$M^+ - 2PF_6$], 459 (30) [$M^+ - 2PF_6$ − py], 258 (5) [M2+ − $2PF_6$]. Anal. Calcd for $C_{21}H_{27}F_{12}N_3P_2RuS_3$: C, 31.19; H, 3.34; N, 5.36. Found: C, 30.77; H, 3.34; N, 5.36.

$[([9]aneS_3)Ru(py)_2(NCMe)][PF_6]_2$, 2. A 0.202 g sample of **1** (0.25 mmol) was dissolved in acetonitrile (10 mL), and the solution was stirred for 2 weeks. The volume of the reaction mixture was then reduced (ca. 5 mL), and the concentrate was added to ethanol (20 mL), giving 0.16 g of **2** (83%) as a pale green powder after drying in vacuo. ^{1}H NMR ($(CD_3)_2CO$): δ 2.70 (s, 3H), 2.90−3.30 (m, 12H), 7.52−7.62 (m, 4H), 8.08 (tt, J = 7.63 and 1.53, 2H), 8.82 (dd, J = 6.43 and 1.53, 4H). FAB MS, *m*/*z* (%): 626 (25) [$M^+ - PF_6$], 480 (10) [$M^+ - 2PF_6$]. Anal. Calcd for $C_{18}H_{25}F_{12}N_3P_2RuS_3$: C, 28.05; H, 3.25; N, 5.45. Found: C, 28.45; H, 3.03; N, 5.54.

$[([9]aneS_3)Ru(py)(NCMe)_2][PF_6]_2$, 3. A 0.202 g sample of **1** (0.25 mmol) was dissolved in acetonitrile (20 mL), and the solution was refluxed for 3 days. The volume of the reaction mixture was then reduced (ca. 5 mL), and the concentrate was added to ethanol (20 mL), yielding 0.14 g of **3** (77%) as a white powder after drying in vacuo. ^{1}H NMR ($(CD_3)_2CO$): δ 2.80 (s, 6H), 2.88−3.20 (m, 12H), 7.61−7.68 (m, 2H), 8.10 (tt, J = 7.50 and 1.53, 1H), 8.98 (dd, J = 6.73 and 1.53, 2H). FAB MS, *m*/*z* (%): 588 (60) [$M^+ - PF_6$]. Anal. Calcd for $C_{15}H_{23}F_{12}N_3P_2RuS_3$: C, 24.59; H, 3.14; N, 5.74. Found: C, 24.31; H, 3.17; N, 5.58.

$[([9]aneS_3)Ru(4,4'\text{-bipy})_3][PF_6]_2$, 4. To a solution of 0.215 g (0.5 mmol) of $[Ru(DMSO)Cl_2([9]aneS_3)]$ in 20 mL of 1:1 ethanol/water was added $AgNO_3$ (0.170 g, 2 equiv), and the reaction mixture was refluxed for 3 h. After filtration and removal of the AgCl precipitate, excess 4,4′-bipyridine (1 g) was added to the filtrate and the mixture was refluxed for a further 3 h. The mixture was then added to 100 mL of water containing NH_4PF_6 (0.245 g, 3 equiv), and the resultant mixture was left overnight to form a precipitate. The crude product was washed sequentially with water and ethanol and then dried in vacuo to yield 0.34 g of **4** as a yellow-orange powder (65%). ^{1}H NMR (CD_3NO_2): δ_H 2.97 (s, 12H), 7.73 (dd, J = 4.58 and 1.53, 6H), 7.89 (dd, J = 5.48 and 1.53, 6H), 8.68−8.76 (m, 12H). FAB MS, *m*/*z* (%): 895 (20) [$M^+ - PF_6$], 747 (10) [$M^+ - 2PF_6$], 593 (10) [$M^+ - 2PF_6$ − bpy]. Anal. Calcd for $C_{36}H_{42}F_{12}N_6O_3P_2RuS_3$ (**4**·$3H_2O$): C, 39.52; H, 3.84; N, 7.68. Found: C, 39.15; H, 3.27; N, 7.45.

$[([9]aneS_3)Ru(4,4'\text{-bipy})_2(NCMe)][PF_6]_2$, 5. A 0.145 g sample of **4** (0.16 mmol) was stirred in acetonitrile (20 mL) for 2 weeks. The volume of the mixture was then reduced by half, and excess ethanol was added to yield 107 mg (72%) of **5** as a green powder after drying in vacuo. ^{1}H NMR (CD_3CN): δ_H 2.40 (s, 3H), 2.51−3.02 (m, 12H), 7.71 (dd, J = 4.58 and 1.53, 4H), 7.79 (dd, J = 5.50 and 1.53, 4H), 8.68 (dd, J = 5.20 and 1.23, 4H), 8.75 (dd, J = 4.28 and 1.53, 4H). FAB MS, *m*/*z* (%): 779 (40) [$M^+ - PF_6$], 634 (18) [$M^+ - 2PF_6$], 593 (10) [$M^+ - 2PF_6$ − NCMe], 478 (12) [$M^+ - 2PF_6$ − bpy]. Anal. Calcd for $C_{28}H_{40}F_{12}N_5O_{4.5}P_2RuS_3$ (**5**·$4.5H_2O$): C, 33.43; H, 3.98; N, 6.97. Found: C, 33.12; H, 3.44; N, 7.10.

$[([9]aneS_3)Ru(4,4'\text{-bipy})(NCMe)_2][PF_6]_2$, 6. A 0.104 g sample of **4** (0.1 mmol) was refluxed in acetonitrile (20 mL) for 3 days. The volume of the mixture was then reduced by half, and ethanol was added to yield 35 mg (43%) of **6** as a pale green powder after drying in vacuo. ^{1}H NMR (CD_3CN): δ_H 2.40 (s, 6H), 2.50−3.00 (m, 12H), 7.73 (dd, J = 4.58 and 1.53, 2H), 7.86 (dd, J = 5.18 and 1.53, 2H), 8.76 (dd, J = 4.58 and 1.53, 2H), 8.84 (dd, J = 5.20 and 1.53, 2H). FAB MS, *m*/*z* (%): 665 (65) [$M^+ - PF_6$], 613 (20) [$M^+ - PF_6$ − NCMe], 519 (20) [$M^+ - 2PF_6$], 478 (20) [$M^+ - 2PF_6$ − NCMe], 437 (20) [$M^+ - 2PF_6$ − 2NCMe]. Anal. Calcd for $C_{20}H_{30}F_{12}N_4O_2P_2RuS_3$ (**6**·$2H_2O$): C, 28.40; H, 3.55; N, 6.63. Found: C, 28.52; H, 3.21; N, 6.67.

$[([9]aneS_3)Ru(NCC_6H_5)_3][PF_6]_2$, 7. To a solution of 0.215 g (0.5 mmol) of $[Ru(DMSO)Cl_2([9]aneS_3)]$ in 20 mL of propyl alcohol was added $AgNO_3$ (0.17 g, 2 equiv), and the reaction mixture was refluxed for 3 h. After filtration, excess benzonitrile (1 mL) was added to the filtrate and the mixture was refluxed for 3 h. Addition of NH_4PF_6 (0.245 g, 3 equiv) resulted in the formation of a pale green precipitate, which was dried in vacuo to yield 0.12 g (27%) of **7**. ^{1}H NMR (CD_3CN): δ_H 2.65−3.05 (m, 12H), 7.58−7.66 (m, 6H), 7.79 (tt, J = 7.63 and 1.53, 3H), 7.93 (dd, J = 8.50 and 1.53, 6H). FAB MS, *m*/*z* (%): 736 (50) [$M^+ - PF_6$], 590 (15) [$M^+ - 2PF_6$]. Anal. Calcd for $C_{27}H_{27}F_{12}N_3P_2RuS_3$: C, 36.82; H, 3.07; N, 4.77. Found: C, 36.31; H, 3.10; N, 4.74.

$[([9]aneS_3)Ru(NCC_2H_5)_3][PF_6]_2$, 8. To a solution of 0.215 g (0.5 mmol) of $[Ru(DMSO)Cl_2([9]aneS_3)]$ in 20 mL of 1:1 ethanol/water was added $AgNO_3$ (0.17 g, 2 equiv), and the reaction mixture was refluxed for 3 h. After removal of AgCl by filtration, excess propionitrile (1 mL) was added and the mixture was refluxed for 3 h. After cooling, NH_4PF_6 (0.245 g, 3 equiv) was added, resulting in a precipitate, which was washed sequentially with water and ethanol and then dried in vacuo to yield 0.21 g (57%) of **8** as a white powder. ^{1}H NMR ($(CD_3)_2CO$): δ_H 1.35 (t, J = 7.30, 9H), 2.50−3.55 (m, 18H). FAB MS, *m*/*z* (%): 592 (45) [$M^+ - PF_6$], 537 (5) [$M^+ - PF_6 - NCC_2H_5$], 447 (15) [$M^+ - 2PF_6$], 427 (5) [$M^+ - PF_6 - 3NCC_2H_5$], 391 (90) [$M^+ - 2PF_6 - NCC_2H_5$], 336 (15) [$M^+ - 2PF_6 - 2NCC_2H_5$]. Anal. Calcd for $C_{15}H_{27}F_{12}N_3P_2RuS_3$: C, 24.46; H, 3.67; N, 5.71. Found: C, 24.23; H, 3.69; N, 5.49.

$[Ru(4,4'\text{-bipy})_2(NCC_2H_5)([9]aneS_3)][PF_6]_2$, 9. A 0.114 g sample of **5** (0.11 mmol) was dissolved in propionitrile (5 mL), and the solution was stirred for 2 weeks. The reaction mixture was then added to diethyl ether (200 mL) to yield 87 mg (85%) of **9** as an orange powder after drying in vacuo. ^{1}H NMR ($(CD_3)_2CO$): δ_H 1.43 (t, J = 7.30, 3H), 2.95−3.30 (m, 14H), 7.78 (dd, J = 4.58 and 1.53, 4H), 7.79 (dd, J = 5.18 and 1.53, 4H), 8.75 (dd, J = 4.58 and 1.53, 4H), 8.99 (dd, J = 5.50 and 1.53, 4H). FAB MS, *m*/*z* (%): 794 (50) [$M^+ - PF_6$], 648 (20) [$M^+ - 2PF_6$]. Anal. Calcd for $C_{29}H_{37}F_{12}N_5O_2P_2RuS_3$ (**9**·$2H_2O$): C, 35.69; H, 3.79; N, 7.12. Found: C, 35.99; H, 3.75; N, 6.88.

$[Ru(4,4'\text{-bipy})(NCC_2H_5)_2([9]aneS_3)][PF_6]_2$, 10. A 0.114 g sample of **5** (0.11 mmol) was dissolved in propionitrile (5 mL), and the solution was refluxed for 3 days. The reaction mixture was then added to diethyl ether (200 mL) to yield 80 mg (87%) of **10** as an orange powder after drying in vacuo. ^{1}H NMR ($(CD_3)_2CO$): δ_H 1.34 (t, J = 7.30, 6H), 2.50−3.20 (m, 16H), 7.75−8.00 (m, 4H), 8.75−9.05 (m, 4H). FAB MS, *m*/*z* (%): 694 (10) [$M^+ - PF_6$], 429 (10) [$M^+ - PF_6$ − bpy −

Table 1. Crystal Data and Structural Refinement Details[a]

	1[b]	**2**[c]	**3**[d]
empirical formula	$C_{22}H_{30}F_{12}N_4O_2P_2RuS_3$[e]	$C_{18}H_{25}F_{12}N_3P_2RuS_3$	$C_{15}H_{23}F_{12}N_3P_2RuS_3$
fw	869.69	770.60	732.55
space group	*Cc*	$P\bar{1}$	$Pna2_1$
λ (Å)	0.710 73	0.710 73	0.710 73
temp (K)	150(2)	150(2)	293(2)
a (Å)	23.267(5)	11.3958(19)	14.748(5)
b (Å)	11.5457(18)	11.4280(19)	18.037(18)
c (Å)	26.192(5)	11.930(2)	10.341(5)
α (deg)	90	100.518(3)	90
β (deg)	114.836(10)	100.542(3)	90
γ (deg)	90	112.493(3)	90
V (Å$^{3)}$	6385(2)	1355.6(4)	2750.8(18)
Z	8	2	4
ρ_{calc} (Mg/m^3)	1.809	1.888	1.769
μ (mm^{-1})	0.888	1.026	1.006
final *R* indices: R1, wR2	0.0370, 0.1013	0.0523, 0.1536	0.0514, 0.1510

[a] $R1 = \sum||F_o| - |F_c||/\sum|F_o|$ and $wR2 = [\sum w(F_o^2 - F_o^2)^2/\sum w(F_o^2)^2]^{1/2}$. [b] $w = 1/[\sigma^2(F_o^2) + (0.0628P)^2 + 0.00P]$. [c] $w = 1/[\sigma^2(F_o^2) + (0.0964P)^2 + 0.00P]$. [d] $w = 1/[\sigma^2(F_o^2) + (0.1029P)^2 + 1.905P]$. [e] Empirical formula for **1**·CH_3NO_2.

$2NCC_2H_5$]. Anal. Calcd for $C_{22}H_{34}F_{12}N_4O_2P_2RuS_3$ (**10**·$2H_2O$): C, 30.24; H, 3.89; N, 6.41. Found: C, 30.01; H, 3.62; N, 5.86.

[Ru(py)$_2$(NCC$_2$H$_5$)([9]aneS$_3$)][PF$_6$]$_2$, 11. A 0.202 g sample of **1** (0.25 mmol) was dissolved in propionitrile (5 mL), and the solution was stirred for 2 weeks. The reaction mixture was then added to diethyl ether (200 mL) to yield 110 mg (56%) of **11** as a white powder after drying in vacuo. ^{1}H NMR (CD_3NO_2): δ_H 1.38 (t, $J = 7.63$, 3H), 2.75−3.20 (m, 14H), 7.50−7.56 (m, 4H), 8.01 (tt, $J = 7.93$ and 1.23, 2H), 8.67 (dd, $J = 6.40$ and 1.23, 4H). FAB MS, *m*/*z* (%): 640 (45) [$M^+ - PF_6$], 495 (20) [$M^+ - 2PF_6$]. Anal. Calcd for $C_{19}H_{27}F_{12}N_3P_2RuS_3$: C, 29.08; H, 3.44; N, 5.36. Found: C, 29.20; H, 3.36; N, 5.37.

[Ru(py)(NCC$_2$H$_5$)$_2$([9]aneS$_3$)][PF$_6$]$_2$, 12. A 0.202 g sample of **1** (0.25 mmol) was dissolved in propionitrile (5 mL), and the solution was refluxed for 3 days. The reaction mixture was then added to diethyl ether (200 mL) to yield 85.5 mg (45%) of **12** as a light green powder after drying in vacuo. ^{1}H NMR ($(CD_3)_2CO$): δ_H 1.43 (t, $J = 7.63$, 6H), 2.80−3.30 (m, 16H), 7.60 (d, $J = 6.40$, 2H), 8.09 (d, $J = 7.63$, H), 8.80 (d, $J = 4.28$, 2H). FAB MS, *m*/*z* (%): 616 (90) [$M^+ - PF_6$], 470 (15) [$M^+ - 2PF_6$], 415 (25) [$M^+ - 2PF_6 - NCC_2H_5$]. Anal. Calcd for $C_{18}H_{28}F_{12}N_{3.2}P_2RuS_3$ (**12**·0.5py): C, 27.84; H, 3.61; N, 5.77. Found: C, 27.50; H, 3.62; N, 5.21.

[([9]aneS$_3$)Ru(py)$_2$Cl][PF$_6$], 13. To a solution of 0.215 g (0.5 mmol) of [Ru(DMSO)Cl$_2$([9]aneS$_3$)] in 20 mL of 1:1 ethanol/water was added excess pyridine (1 mL), and the mixture was stirred at reflux for 3 h. After cooling, NH_4PF_6 (0.165 g, 2 equiv) was added, resulting in a precipitate, which was washed sequentially with water and ethanol and then dried in vacuo to yield 0.170 g (55%) of **13** as a yellow powder. ^{1}H NMR (CD_3CN): δ_H 2.65−3.20 (m, 12H), 7.40−7.55 (m, 4H), 7.90−8.05 (m, 2H), 9.00 (dd, $J = 6.40$ and 1.53, 4H). FAB MS, *m*/*z* (%): 477 (20) [$M^+ - PF_6$], 443 (10) [$M^+ - PF_6 - Cl$]. Anal. Calcd for $C_{16}H_{25}ClF_6N_2O_{1.5}PRuS_3$ (**13**·$1.5H_2O$): C, 31.19; H, 3.34; N, 5.36. Found: C, 30.77; H, 3.34; N, 5.36.

[([9]aneS$_3$)Ru(4,4′-bipy)$_2$Cl][PF$_6$], 14. To a solution of 0.215 g (0.5 mmol) of [Ru(DMSO)Cl$_2$([9]aneS$_3$)] in 20 mL of 1:1 ethanol/water was added excess 4,4′-bipyridine (1 g), and the mixture was stirred at reflux for 3 h. After cooling, NH_4PF_6 (0.165 g, 2 equiv) was added, resulting in a precipitate, which was washed sequentially with water and ethanol and then dried in vacuo to yield 0.25 g (65%) of **14** as an orange powder. ^{1}H NMR ($(CD_3)_2CO$): δ_H 2.70−3.40 (m, 12H), 7.75−7.90 (m, 8H), 8.74 (dd, $J = 4.58$ and 1.83, 4H), 9.19 (dd, $J = 5.18$ and 1.53, 4H). FAB MS, *m*/*z* (%): 629 (60) [$M^+ - PF_6$], 472 (15) [$M^+ - PF_6 -$ bipy]. Anal. Calcd for $C_{26}H_{28}ClF_6N_4PRuS_3$: C, 40.31; H, 3.62; N, 7.24. Found: C, 40.01; H, 3.34; N, 7.01.

[([9]aneS$_3$)Ru(4,4′-bipy)$_2$(py)][PF$_6$], 15. To a solution of 0.365 g (0.47 mmol) of [([9]aneS$_3$)Ru(4,4′-bipy)$_2$Cl][PF$_6$] in 10 mL of nitromethane was added $AgPF_6$ (0.139 g, 1 equiv), and the reaction mixture was refluxed for 3 h. After removal of the AgCl precipitate, excess pyridine (1 mL) was added to the filtrate and the mixture was refluxed for a further 3 h. The solvent level was then reduced to 5 mL, and the concentrate was added to ca. 250 mL of diethyl ether to yield 0.165 g (36%) of **17** as an orange powder after drying in vacuo. ^{1}H NMR ($(CD_3)_2CO$): δ_H 2.90−3.20 (m, 12H), 7.55−7.67 (m, 4H), 7.80 (dd, $J = 4.58$ and 1.53, 2H), 7.93−8.02 (m, 4H), 8.08−8.13 (m, 1H), 8.62−8.78 (m, 10H). FAB MS, *m*/*z* (%): 817 (10) [$M^+ - PF_6$], 738 (10) [$M^+ - PF_6 -$ py], 661 (70) [$M^+ - PF_6 -$ bipy], 592 (15) [$M^+ - 2PF_6 -$ py], 518 (30) [$M^+ - 2PF_6 -$ bipy]. Anal. Calcd for $C_{31}H_{43}F_{12}N_5O_{1.5}P_2RuS_3$: C, 35.36; H, 4.08; N, 6.65. Found: C, 34.96; H, 3.48; N, 5.99.

X-ray Structures of 1 and 2. Crystals of **1** were obtained by vapor diffusion from a nitromethane and diethyl ether mixture. Crystals of **2** were grown by vapor diffusion from an acetone and diethyl ether mixture. Crystals of each complex were mounted on a thin glass fiber with Teflon oil and placed on a Bruker Smart CCD area detector with an Oxford Cryosystems low-temperature system. Cell parameters were refined from the setting angles of 224 reflections (θ range $1.71 < \theta < 28.28°$) for **1** and 69 reflections (θ range $1.78 < \theta < 28.34°$) for **2**. Reflections were measured from a hemisphere of data from frames each covering 0.3° in ω. All reflections measured were corrected for Lorentz and polarization effects and for absorption by semiempirical methods based on symmetry-equivalent and repeated reflections. The structures were solved by direct methods[16] and refined by full-matrix least-squares methods on F^2. Hydrogen atoms were placed geometrically and refined with a riding model and with U_{iso} values constrained to be 1.2 times the U_{eq} values of the carrier atoms. Complex scattering factors were taken from the program package SHELXTL[16] as implemented on the Viglen Pentium computer.

X-ray Structure of 3. Crystals of **3** were grown by vapor diffusion from an acetone and diethyl ether mixture. A crystal of **3** was mounted on a thin glass fiber using epoxy resin and placed at room temperature on a Siemens P4 diffractometer. Data were collected in the range $3.5 < 2\theta < 50°$. All reflections measured were corrected for Lorentz and polarization effects (but not for absorption). The structure was solved by direct methods[17] and refined by full-matrix least-squares methods on F^2. Hydrogen atoms were included in calculated positions and refined in the riding mode. Complex scattering factors were taken from the program package SHELXL93[17] as implemented on the Viglen 486 dx computer.

Crystallographic data and refinement details are presented in Table 1.

Results and Discussion

Syntheses. 1 was synthesized by a method analogous to that used for the synthesis of [Ru(NCMe)$_3$([9]aneS$_3$)]$^{2+}$. An X-ray

(16) *SHELXTL: an integrated system for solving and refining crystal structures from diffraction data*, Revision 5.1; Bruker AXS Ltd.
(17) Sheldrick, G. M. *SHELXL93: an integrated system for solving and refining crystal structures from diffraction data*; University of Göttingen: Göttingen, Germany, 1993.

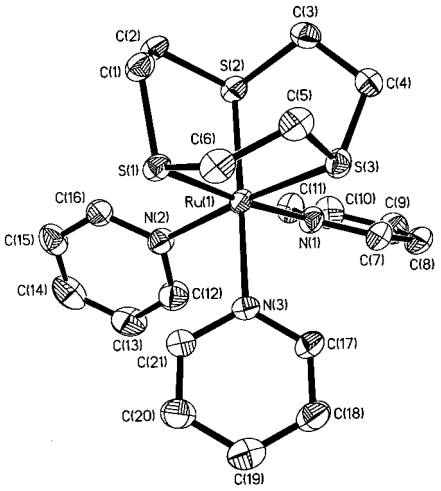

Figure 1. Structural representation of the cation in **1**, $[Ru(py)_3([9]aneS_3)]^{2+}$, with hydrogen atoms omitted. The thermal ellipsoids correspond to 50% probability.

diffraction study on a crystal of **1** confirmed the postulated structure (Figure 1).

Although **1** is stable in solvents such as nitromethane and dichloromethane, it is unstable toward solvolysis in more coordinating solvents. Models and the X-ray data confirm that one face of the complex is sterically congested due to interactions between the ortho hydrogens of the coordinated pyridine ligands. It was reasoned that these unfavorable steric interactions are the cause of the relative instability of **1**. In fact, these interactions mean that **1** is a suitable starting material for the synthesis of heteroleptic ruthenium(II) complexes. In many cases, Ru(II) complexes incorporating pyridine ligands are synthesized via nitrile intermediates.[18] However, in this case, the opposite is true. The pyridyl ligands of **1** may be substituted by suitable nitrile ligands.

Our initial studies involved stirring **1** in the coordinating solvent acetonitrile (MeCN) at room temperature. ^{1}H NMR spectroscopy clearly showed that, after 2 weeks, **1** was cleanly converted into the bis(pyridyl) complex $[Ru(py)_2(NCMe)([9]aneS_3)][PF_6]_2$, **2**, and uncoordinated pyridine. **2** was isolated as a analytically pure product by simple precipitation with ethanol. An X-ray diffraction study on a crystal of **2** confirmed the postulated structure. An analysis of the structural data revealed disorder of both the cation and the anions. However, this was satisfactorily modeled to confirm the postulated structure of **2** (Figure 2).

The reactivity of **1** under more forcing conditions was investigated. **1** was dissolved in MeCN, and this reaction mixture was brought to reflux. Again, the reaction was monitored by ^{1}H NMR spectroscopy. These studies clearly showed that, after 3 days, **1** was converted into the mono(pyridyl) complex $[Ru(py)(NCMe)_2([9]aneS_3)][PF_6]_2$, **3**. This complex was also isolated as an analytically pure product by simple precipitation with ethanol. An X-ray diffraction study on a crystal of **3** confirmed the expected structure Again, an analysis of the structural data revealed disorder of both the cation and the anions. However, this was satisfactorily modeled to confirm the postulated structure of **3** (Figure 3).

Since **3** only incorporates one coordinated pyridyl ligand, it was postulated that, because all possible unfavorable hydrogen

(18) See, for example: (a) Onishi, M.; Ikemoto, K.; Hiraki, K. *Inorg. Chim. Acta* **1994**, *219*, 3. (b) Bossard, G. E.; Abrahams, M. J.; Darkes, M. C.; Vollano, J. F.; Brooks, R. C. *Inorg. Chem.* **1995**, *34*, 1524.

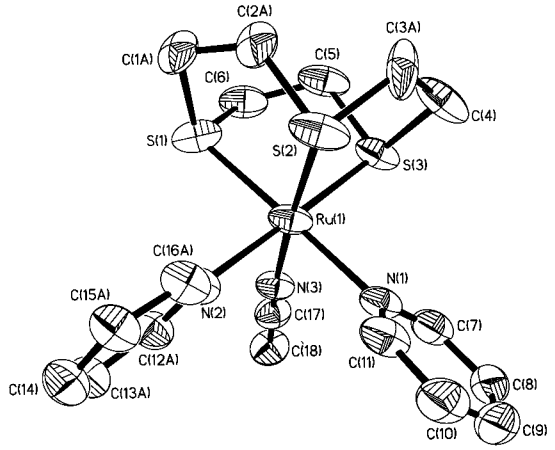

Figure 2. Structural representation of the cation in **2**, $[Ru(py)_2(NCMe)([9]aneS_3)]^{2+}$, with hydrogen atoms omitted. The thermal ellipsoids correspond to 50% probability.

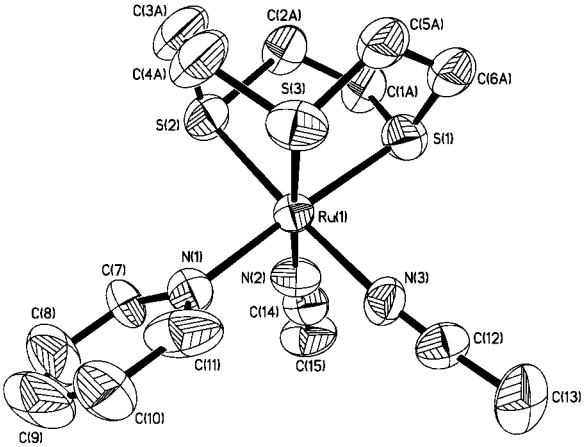

Figure 3. Structural representation of the cation in **3**, $[Ru(py)(NCMe)_2([9]aneS_3)]^{2+}$, with hydrogen atoms omitted. The thermal ellipsoids correspond to 50% probability.

interactions between coordinated ligands had been removed, **3** would be stable toward substitution reactions. This was confirmed by the observation that **3** is stable in refluxing acetonitrile and no reaction was observed over several weeks.

Further proof that steric interactions are the driving force for such reactions is provided by the synthesis of $[Ru(NCPh)_3([9]aneS_3)][PF_6]_2$, **7** (where PhCN is benzonitrile). Compared to the case of **1**, any steric interaction in **7** should be reduced, as the aromatic rings are lifted away from the face of the metal ion. Experimental evidence confirms this hypothesis: both **7** and $[Ru(NCMe)_3([9]aneS_3)]^{2+}$ [15] are inert to solvolysis by other coordinating solvents, even over a period of 1 month.

This reaction scheme outlined above has a more general application: other pyridyl and nitrile ligands take part in analogous reactions (Scheme 1). For example, we have employed 4,4′-bipyridine (4,4′-bipy) instead of pyridine to synthesize the complex $[Ru(4,4'\text{-bipy})_3([9]aneS_3)][PF_6]_2$, **4**. Again, solvolysis occurs, and depending on the reaction conditions, the complex $[Ru(4,4'\text{-bipy})_2(NCMe)([9]aneS_3)][PF_6]_2$, **5**, or $[Ru(4,4'\text{-bipy})(NCMe)_2([9]aneS_3)][PF_6]_2$, **6**, can be isolated as an analytically pure product by simple precipitation. Scheme 1 is also applicable to different nitrile ligands. Using very similar reaction conditions, for example, we have isolated $[Ru(4,4'\text{-bipy})_2(NCC_2H_5)([9]aneS_3)][PF_6]_2$, **9**, and $[Ru(py)(NCC_2H_5)_2([9]aneS_3)][PF_6]_2$, **12**. All of these compounds have been characterized by ^{1}H NMR spectroscopy, UV/vis spectroscopy, mass spectroscopy, elemental analysis, and electrochemistry.

Scheme 1

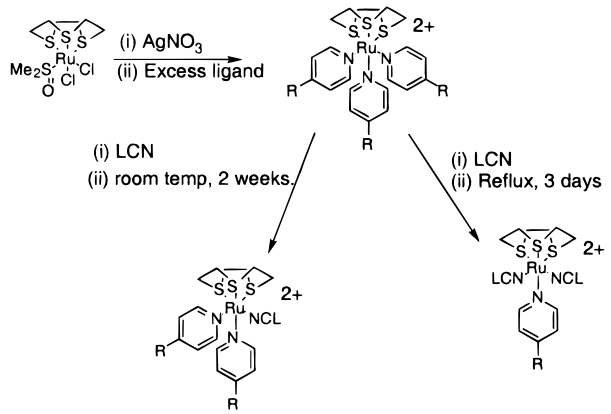

Scheme 2

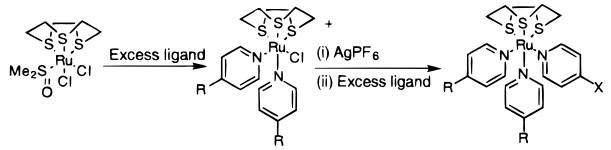

Heteroleptic compounds incorporating different pyridyl-based ligands can also be synthesized via an alternative route. If $[Ru(DMSO)Cl_2([9]aneS_3)]$ is not treated with silver nitrate, then reactions with pyridyl ligands yield bis-substituted products such as $[Ru(4,4'\text{-bipy})_2Cl([9]aneS_3)][PF_6]$, **14**. Presumably, the formation of these monocationic species is due to the restricted ability of thioethers to neutralize positive charges through σ-donation.[19,20] Treatment of **14** with 1 equiv of Ag^+ in a noncoordinating solvent followed by addition of a suitable pyridyl ligand yields a heteroleptic complex, such as $[Ru(4,4'\text{-bipy})_2(py)([9]aneS_3)][PF_6]$, **15**, which incorporates two different pyridyl ligands (Scheme 2). ^{1}H NMR spectroscopy, FAB MS mass spectroscopy, UV/visible spectroscopy, and elemental analysis all indicate that, using this procedure, the targeted structures are the only products synthesized and no ligand scrambling is observed.

UV/Visible Absorption Spectroscopy. The UV/visible spectra of the new complexes and $[Ru(NCMe)_3([9]aneS_3)]^{2+}$ [15] were recorded in acetonitrile. As the data in Table 2 show, many of the complexes display similar features in their spectra.

In all cases, intense high-energy transitions are observed. For example, complexes incorporating py ligands (**1**, **2**, **3**, **11**, **12**, **13**, and **15**) all show a band at 220−250 nm. The intensity of this band is dependent on the number of coordinated py ligands and is assigned as a ligand-centered (LC) py $\pi-\pi^*$ transition. These complexes also display an intense band between 275 and 310 nm. The intensity of this band is also dependent on the number such ligands coordinated to the metal center. The position and intensity of this band are consistent with Ru(d) → py(π^*) metal-to-ligand charge transfer (MLCT).[21]

Similarly, complexes incorporating bipy ligands (**4**, **5**, **6**, **9**, **10**, **14**, and **15**) show bands at 240−246 and 320−365 nm. The intensitues of both bands are dependent on the number of coordinated bipy ligands. Again, the positions and intensities of these bands are consistent with LC bpy $\pi-\pi^*$ and MLCT Ru(d) → bpy(π^*) transitions, respectively.[21]

Table 2. UV/Vis Data

complex	λ_{max} (nm)	ϵ (M^{-1} cm^{-1})	complex	λ_{max} (nm)	ϵ (M^{-1} cm^{-1})
1	240	8655	**9**	243	35462
	303	10317		330	13132
2	236	8560	**10**	241	24998
	301	9728		324	9746
3	228	8133	**11**	240	7551
	297	5945		295	8551
4	244	50101	**12**	225	10154
	336	18473		296	7742
5	244	37040	**13**	240	8104
	280	22463		309	3782
	323	13223	**14**	244	31373
6	242	20514		361	10827
	271	15747	**15**	240	21774
	325	7801		303	7391
7	222	81250	$[Ru(DMSO)\text{-}Cl_2([9]aneS_3)]$	215	22321
	263	11850		386	786
	340	333	$[Ru(NCMe)_3\text{-}([9]aneS_3)]^{2+}$	207	24079
8	216	9781		271	4366
	300	323		336	1076
	344	817			

Table 3. Electrochemical Data

compound	$E_{1/2}$ (V)[a]	ΔE_p (mV)	E_p (V)[b]
$[Ru(DMSO)Cl_2([9]aneS_3)]$	0.943	82	
$[Ru(NCMe)_3([9]aneS_3)]^{2+}$	1.909	68	
1	1.667	69	
2	1.752	99	
3	1.791	113	
4			1.680
5			1.744
6			1.759
7			2.007
8			1.983
9			1.750
10			1.782
11	1.705	115	
12	1.798	118	
13	1.243	114	
14	1.254	98	
15	1.660	94	

[a] Vs Ag/AgCl. [b] Complexes are not fully chemically reversible; therefore, only E_p values are quoted.

The UV/vis data for complexes incorporating nitrile ligands all show three transitions. The most intense transition at 205−225 nm (ϵ = 6000−81 500 M^{-1} cm^{-1}) is dependent on the number of nitrile ligands coordinated to the ruthenium metal center and, by comparison to similar complexes,[22,23] has been assigned as an MLCT Ru(d) → nitrile(π^*) transition. Two transitions at 260−300 nm (ϵ = 200−12 000 nm M^{-1} cm^{-1}) and 335−375 nm (ϵ = 300−850 M^{-1} cm^{-1}) are also observed. The positions and intensities of these bands are consistent with spin-allowed, Laporte-forbidden, $t_{2g}^6(^1A_{1g}) \rightarrow t_{2g}^5e_g$ ($^1T_{1g}$, $^1T_{2g}$) d−d transitions.[22,23]

Electrochemistry. The electrochemistry of the new complexes was investigated using cyclic voltammetry. Apart from the expected ligand reduction couples, the cyclic voltammograms of the complexes all display oxidations associated with the d^5/d^6 Ru(III)/Ru(II) couple (Table 3). An analysis of these couples using variable sweep rates and convolution/deconvolution techniques[24] reveals that, while all the oxidations are

(19) Brandt, K.; Sheldrick, W. S. *J. Chem. Soc., Dalton Trans.* **1996**, 1237.
(20) Young, I. R.; Ochrymowycz, L. A.; Rorabacher, D. B. *Inorg. Chem.* **1986**, *25*, 2576.
(21) Haga, M.; Dodsworth, E. S.; Lever, A. B. P. *Inorg. Chem.* **1986**, *25*, 447.
(22) Fantucci, P. C.; Valenti, V.; Cariati, F. *Inorg. Chim. Acta* **1971**, 425.
(23) Gray, H. B.; Beach, N. A. *J. Am. Chem. Soc.* **1963**, *85*, 2922.
(24) Bard, A. J.; Faulkner, L. R. *Electrochemical Methods. Fundamentals and Applications*; John Wiley and Sons: New York, 1980; pp 236−241.

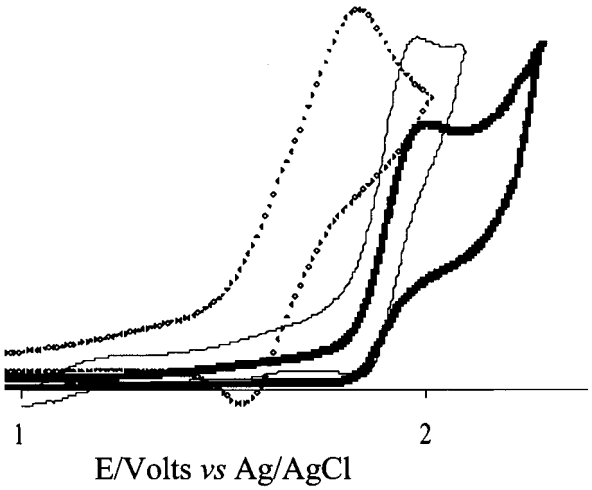

Figure 4. A comparison of oxidation processes observed for **4** (◊), **7** (■), and $[Ru(NCMe)_3([9]aneS_3)][(PF_6)_2]$ (—).

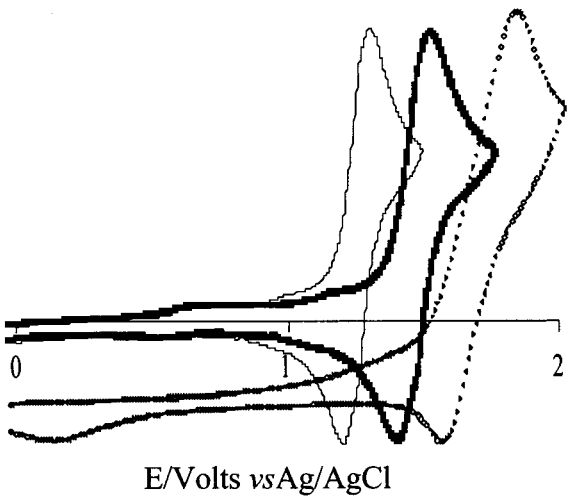

Figure 5. A comparison of oxidation processes observed for $[Ru(DMSO)Cl_2([9]aneS_3)]$ (—), **14** (■), and **4** (◊).

electrochemically reversible, several complexes display oxidation couples which are not chemically reversible. Therefore, E_p is quoted in these cases. It is known that nitrile complexes of Ru(III) undergo facile hydrolysis.[25] Hence, there is a possibility that this observed chemical irreversibility is due to hydrolysis by adventitious water. However, the electrochemistry of each complex was investigated several times and consistent results were obtained.

A comparison of the electrochemistry of complexes such as **4**, **7**, and $[Ru(NCMe)_3([9]aneS_3)][PF_6]_2$, which are homoleptic with respect to all three metal coordinated N-donor ligands, reveals a consistent trend (Figure 4).

When py is the coordinated ligand, as in **1**, the Ru(III)/Ru(II) couple is observed at 1.67 V. A slightly more anodic Ru(III)/Ru(II) couple is observed for **4**, where the oxidation occurs at 1.68 V. This is due to the similar σ-donor/π-acceptor properties of py and bpy ligands. However, when the ligand is changed to a nitrile, a much larger anodic shift in the Ru(III)/Ru(II) couple is observed. For $[Ru(NCMe)_3([9]aneS_3)]^{2+}$ $E_{1/2} = 1.91$ V, while for **8** (where L = EtCN) $E_1 = 1.98$ V and for **7** (where L = benzonitrile) $E_1 = 2.01$ V. These results are consistent with previous comparisons made between pyridyl and nitrile ligands, which have shown that pyridyl ligands are better σ-donors[26] but poorer π-acceptors[27] than nitriles and that benzonitrile is a better π-acceptor ligand than acetonitrile.[28]

As the data in Table 2 show, the Ru(III)/Ru(II) couples of complexes incorporating mixed py and nitrile ligands show a less pronounced but, nevertheless, analogous trend, thus allowing the Ru(III)/Ru(II) couple to be shifted by smaller increments. For example, as the py ligands of **1** are substituted with acetonitrile ligands to form **2** and **3**, the ruthenium(II) oxidation becomes progressively more anodic. The same trend is also seen when propionitrile—which has similar donor/acceptor properties—is used as the nitrile ligand.

It is also possible to induce shifts in the Ru(III)/Ru(II) couple using π-donor ligands. Figure 5 shows a comparison of the oxidation couples for $[Ru(DMSO)Cl_2([9]aneS_3)]$, **14**, and **4**. From the diagram it can be seen that, as the number of π-donor chloride ligands coordinated to the metal center increases, the Ru(III)/Ru(II) couple shows the expected cathodic shift.

Conclusions. By exploiting unfavorable interactions between coordinated pyridyl ligands and the restricted ability of thioethers to neutralize positive charges on metal complexes, we found that it is possible to control the substitution chemistry of the $[Ru([9]aneS_3)]^{2+}$ fragment. This has led to a general method for the facile synthesis of heteroleptic complexes incorporating this fragment and facially coordinated N-donor ligands. All the reported complexes incorporating this metal center display metal-localized oxidations. By variation of the N-donor ligand set, it is possible to shift the Ru(III)/Ru(II) couple by >300 mV. Incorporation of π-donor ligands into such complexes leads to even greater shifts.

Work in this laboratory is now centering on mono- and oligometallic complexes incorporating a variety of S-donor ligand sets. Future work will center on exploiting these complexes and synthetic methodologies to construct more complex functional structures with targeted coordination geometries and electronic properties.

Acknowledgment. J.A.T. thanks The Royal Society for funding and support. S.R. is grateful to the EPSRC for the provision of a research studentship.

Supporting Information Available: X-ray crystallographic files, in CIF format, for **1**−**3**. This material is available free of charge via the Internet at http://pubs/acs/org.

IC991336G

(25) Zanella, A. W.; Ford, P. C. *Inorg. Chem.* **1975**, *14*, 42.
(26) Anderson, W. P.; Brill, T. B.; Schoenberg, A. R.; Stanger, C. W. *J. Organomet. Chem.* **1972**, *44*, 161.
(27) Prados, R. A.; Clausen, C. A.; Good, M. L. *Inorg. Chem.* **1973**, *2*, 201.
(28) Clarke, R. E.; Ford, P. C. *Inorg. Chem.* **1970**, *9*, 227.